*JOURNAL OF NANO- AND ELECTRONIC PHYSICS*
Vol. **11** No 6, 06010(5pp) (2019)

*ЖУРНАЛ НАНО- ТА ЕЛЕКТРОННОЇ ФІЗИКИ*
Том **11** № 6, 06010(5cc) (2019)

# Sintering Temperature Dependent Optical and Vibrational Properties of $Sm_2NiMnO_6$ Nanoparticle

R. Mukherjee[1,*], Md.S. Sheikh[2], T.P. Sinha[2]

[1] *Department of Physics, Ramananda College, Bishnupur, 722122, Bankura, India*
[2] *Department of Physics, Bose Institute, 93/1 A. P. C. Road, 700009 Kolkata, India*

(Received 11 July 2019; revised manuscript received 04 December 2019; published online 13 December 2019)

Double perovskite oxides (DPOs) are interesting materials due to their various important technological properties. Rare earth DPO $Sm_2NiMnO_6$ (SNMO) nanoparticle is prepared by sol gel method. Varying the sintering temperature from 650-950 °C, four types of materials are synthesized. Room temperature X-ray diffraction (XRD) patterns show that all the samples have the highest intensity peak at Bragg angle $2\theta = 33.05°$ approximately. Rietveld refinement of the XRD pattern of the materials shows that all the materials are crystallized in $P2_1/n$ space group. Despite the monoclinic symmetry with the same space group for the samples, there are variations in lattice parameters, crystal volume, bond lengths and bond angles with the change in sintering temperature. The band gap of the materials is obtained using Tauc relation to UV-visible spectra and found to vary from 1.2 to 1.41 eV. The photoluminescence (PL) emission spectra of the sample are measured at various excitation wavelengths. The PL spectra and the emission feature depend on the wavelength of the excitation. Fourier transform infrared (FTIR) spectra of the materials carry the signature of the double perovskite structure. Strong absorption peak at 575 $cm^{-1}$ in the FTIR spectra is due to the combined effect of Ni-O and Mn-O stretching vibration. The Raman spectra of the samples taken at 488 nm wavelength are analyzed to obtain the vibrational modes of the samples. Lorentzian lines are used to fit the Raman spectra. Group theoretical study is performed to assign the different vibrational modes of the samples in accordance with the structural symmetry. Phonon modes appeared at 641 $cm^{-1}$ are due to stretching (breathing) vibration and at 500 $cm^{-1}$ are due to the combination of anti-stretching and bending motion of the $(Ni/Mn)O_6$ octahedra. Variation of the frequency and width of the Raman spectra is correlated with the structural changes of the samples.

**Keywords:** Double perovskite, X-ray diffraction, Rietveld refinement, Raman spectroscopy.

DOI: 10.21272/jnep.11(6).06010 PACS number: 81.07.Wx

## 1. INTRODUCTION

Rare earth DPOs of general formula $RE_2B'B''O_6$ [RE = rare earth, B' and B'' are transition metals] have attracted the attention of scientists because of their properties like ferromagnetic insulator, spin-phonon and magnetoelectric coupling etc. Apart from the B'/B'' cation ordering, the octahedral displacement and distortion within the $B'O_6$ and $B''O_6$ cage cause a dramatic change in structural, electrical and magnetic properties. When the charge difference between the two B-site cations is equal to two or more, there will be a disordered, partially ordered or ordered arrangement depending on the ionic radii of the B' and B'' cations [1]. For ordered arrangement of B' and B'' cations, the parameter $K = |r_{B'} - r_{B''}|/r_{B''} \geq 0.09$, (where $r_{B'}$ and $r_{B''}$ are the ionic radii of B' and B'' cations) to be maintained [2]. Apart from size difference, there should be charge difference of, at least, twice the electronic charges between the two B/B′-cations or electronegativity difference of the B/B′-site cation [3].

Using polarized Raman spectroscopy, Iliev et al. [4] showed high degree of $Ni^{2+}/Mn^{4+}$ ordering in $LaNiMnO_6$. The crystals are heavily twinned at microscopic level and the effect of micro twinning on the Raman spectra has been analyzed. DPOs $Ln_2NiMnO_6$ [Ln = La, Eu, Dy, Lu] are easily synthesizable and they have carrier lifetime very close to Si solar cell and show good photovoltaic performance [5]. The high value of dielectric constant for SNMO at room temperature and normal frequency prohibits the recombination rate of electron-hole pair. Due to low exciton binding energy and low carrier recombination rate, it is a good candidate for photovoltaic and photocatalytic activities [6]. In the previous paper [6], it was shown that SNMO can be used as a promising solar cell absorber material. $NiO_6$ and $MnO_6$ octahedral distortion in SNMO causes remarkable optical anisotropy and strong birefringence [6]. Large calculated value of birefringence at the energy region below the optical band gap indicates that SNMO may be used as a promising material in various non-linear optical applications. The photocatalytic degradation performance under the visible light suggests that SNMO may also take part in the sunlight-induced degradation of the various aquatic pollutants. In this paper, the prepared material was heat treated at different temperatures and different characterization was done to study the effect of temperature on the different properties of the material.

## 2. EXPERIMENTAL

As reported earlier in [6], SNMO nanoparticles were synthesized by the sol-gel method using metal nitrates $Sm(NO_3)_3 \cdot 6H_2O$, $Ni(NO_3)_2 \cdot 4H_2O$ and $Mn(NO_3)_2 \cdot 6H_2O$. The obtained solution was then stirred for 4 h at room temperature by a magnetic stirrer followed by drying at 120 °C until the combustion has taken place to produce a dark fluffy precursor powder. The powder was sintered separately at 650, 750, 850 and 950 °C. Room tempera-

* rajeshxrd@gmail.com

 

ture XRD pattern of the samples was taken by a powder X-ray diffractometer (Rigaku Miniflex-II) with CuKα radiation of wavelength $\lambda \sim 1.54$ Å. The absorption and photoluminescence emission spectra were recorded using UV-visible spectrophotometer (Shimadzu UV-VIS absorption spectrometer) and fluorescence spectro-fluorometer (FP-8500 JASCO), respectively. The lattice parameters and band gap value for the sample SNMO650 are taken from the previous report [6]. The Fourier transform infrared (FTIR) spectrum of the sample was recorded between 350 and 4000 $cm^{-1}$ with a Perkin- Elmer FTIR1000 instrument, using the KBr pellet technique. The room temperature Raman spectrum was collected at an excitation wavelength of 488 nm using a Lab-RAM HR 800 (Jobin Yvon) Raman spectrometer.

## 3. RESULTS AND DISCUSSION

### 3.1 XRD Analysis

The room temperature XRD pattern of SNMO sintered at different temperatures is shown in Fig. 1. All the materials are crystallized in $P2_1/n$ space group. Symbols represent the experimental data and solid line represents the simulated pattern obtained using the Fullprof code [7]. The vertical lines represent the Bragg's positions and the bottom line is the difference between the observed and simulated pattern. The cell parameters, atomic coordinates, interatomic distances and Ni-O-Mn angles are listed in Table 1. Different ions are distributed in different crystallographic positions like $Sm^{3+}$ occupies 4*e* site, $Ni^{2+}$ – 2c site, $Mn^{4+}$ – 2*d* site and three non-equivalent 4e sites for three $O^{2-}$ ions. Transition metal Ni and Mn cations are completely ordered in their respective Wyckoff positions. Each $Ni^{2+}$ and $Mn^{4+}$ ion is surrounded by six $O^{2-}$ ions forming $NiO_6$ and $MnO_6$ octahedra. The Mn and Ni cations are localized in the corner sharing octahedral environment with three different Mn-O and Ni-O distances. The distortion in this double perovskite compound is considered to be due to the cooperative tilting of the $NiO_6$ and $MnO_6$ octahedra along the three axes of the primitive perovskite unit cell. Fig. 2 shows the variation of lattice parameter of SNMO. For sample sintered at 850 °C, there is an abrupt contraction of lattice parameter along with contraction of unit cell volume.

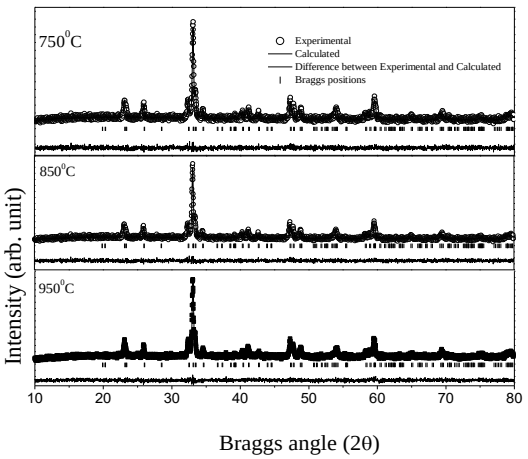


**Fig. 1** – XRD pattern of SNMO synthesized at different temperatures

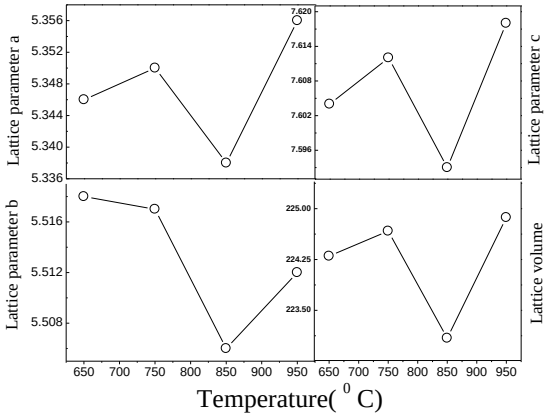


**Fig. 2** – Variation of lattice parameter and cell volume with temperature

**Table 1** – Different parameters obtained from Rietveld refinement

| Sample | Lattice parameter (Å), Volume (Å$^3$) | Bond length (Å) Bond angle (deg.) |
|---|---|---|
| SNMO650 [6] | $a$ = 5.346<br>$b$ = 5.518<br>$c$ = 7.604<br>$\beta$ 90.01<br>$V$ = 224.30 | Ni-O1=1.983<br>Ni-O2=1.916<br>Ni-O3=2.189<br>Mn-O1=1.959<br>Mn-O2=2.014<br>Mn-O3=1.732<br>Ni-O1-Mn=154.05<br>Ni-O2-Mn=155.63<br>Ni-O3-Mn=151.54 |
| SNMO750 | $a$ = 5.350<br>$b$ = 5.517<br>$c$= 7.612<br>$\beta$ = 89.95<br>$V$ = 224.67 | Ni-O1=1.9135<br>Ni-O2=1.9188<br>Ni-O3=2.2134<br>Mn-O1=2.028<br>Mn-O2=2.044<br>Mn-O3=1.717<br>Ni-O1-Mn=154.25<br>Ni-O2-Mn=151.69<br>Ni-O3-Mn=150.80 |
| SNMO850 | $a$ = 5.338<br>$b$ = 5.506<br>$c$ = 7.593<br>$\beta$ = 90.01<br>$V$ = 223.09 | Ni-O1=1.9096<br>Ni-O2=1.9147<br>Ni-O3=2.2076<br>Mn-O1=2.023<br>Mn-O2=2.039<br>Mn-O3=1.714<br>Ni-O1-Mn=154.27<br>Ni-O2-Mn=151.68<br>Ni-O3-Mn=150.79 |
| SNMO950 | $a$ = 5.356<br>$b$ = 5.512<br>$c$ = 7.618<br>$\beta$ = 90.02<br>$V$ = 224.87 | Ni-O1=1.9130<br>Ni-O2=1.9199<br>Ni-O3=2.2146<br>Mn-O1=2.0285<br>Mn-O2=2.0431<br>Mn-O3=1.7192<br>Ni-O1-Mn=154.26<br>Ni-O2-Mn=151.67<br>Ni-O3-Mn=150.79 |

### 3.2 UV-Visible and Photoluminescence Spectroscopy

Fig. 3 shows the UV-visible absorption spectrum of SNMO synthesized at different temperatures. The spectrum exhibits a well-defined absorption feature (peak/hump) due to the optical transition of the first excitonic state. Humps appear at 640, 610, and 490 nm when the sintering temperatures are 950, 850, and 750 °C. As the sintering temperature decreases, the particle size decreases. So, the wavelength of the exciton absorption is blue shifted with the decrease of sintering temperature. This happens due to the quantum confinement of the photogenerated electron-hole pair. The absorption of SNMO nanoparticles starts increasing with the increase of energy near the excitation wavelength of 900 nm. Tauc plot from UV-visible absorption spectrum of the SNMO is shown in Fig. 4. The energy band gap is determined using Tauc relation [8]. A graph is plotted between $(\alpha h\nu)^2$ and $E$ (= $h\nu$). The extrapolation of the linear absorption-edge part of this graph with a straight line to $(\alpha h\nu)^2 = 0$ axis gives the value of the band gap. Here $\alpha$ is the optical adsorption coefficient, $h$ is the Planck constant; $\nu$ is the frequency of light photon. The values of the optical band gap ($E_g$) for direct transition are found to be about 1.2-1.41 eV for the three samples. Band gap decreases with the increase of sintering temperature as shown in the inset of Fig. 4.

Photoluminescence (PL) spectroscopy was also used to characterize the optical property of the SNMO materials synthesized at different temperatures. It can provide information on the presence of native defects, impurities and structural defects. As shown in Fig. 5. SNMO exhibit emission peaks at 300, 325, 380 nm at excitation wavelength of 274 nm and 336, 355, 403 nm at excitation wavelength of 300 nm. The emission response is attributed to band-to-band (or band-edge) transitions, near-band edge emissions and defect-level-emissions. Variation in the excitation wavelength/energy of laser source specifically excites the charge carriers trapped in the localized states nearby valence continuum. Further, the charge carriers undergo recombination process near the conduction continuum and emit light of specific wavelength while coming back to the respective ground states [9]. As the number of particles, taking part in the luminescence process decreases with time, the intensity of the peaks also decreases with the change of the excitation wavelength.

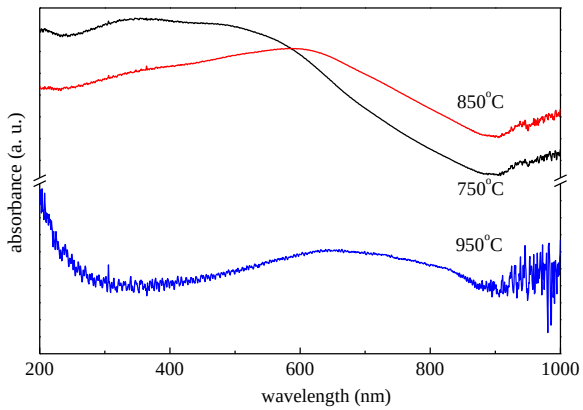


**Fig. 3** – UV-visible absorption spectrum of SNMO

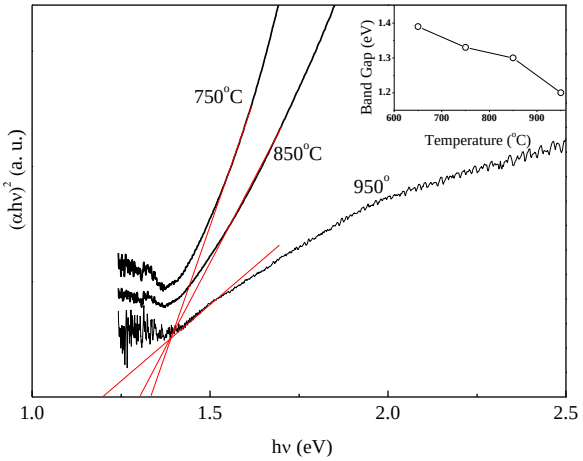


**Fig. 4** – Tauc plot of SNMO at different temperatures. Inset shows variation of bandgap with sintering temperature

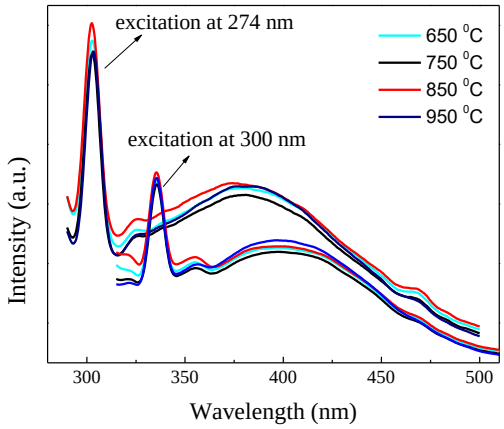


**Fig. 5** – PL spectra at different excitation wavelength of SNMO

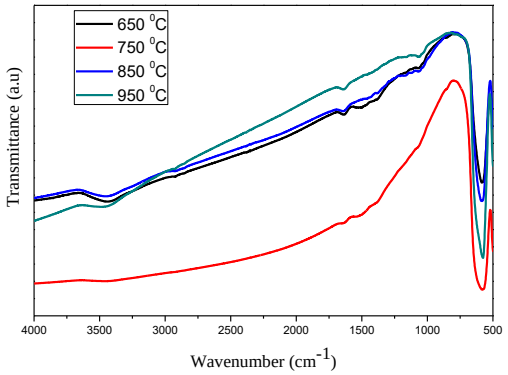


**Fig. 6** – FTIR spectra of SNMO

### 3.3 FTIR and Raman Spectroscopy

Fourier transform infrared (FTIR) spectroscopy is used to know the phase composition and phase purity of the prepared material. All the peaks are the characteristics of the materials. In Fig. 6, we see that a weak peak at 3430 $cm^{-1}$ is referred to stretching vibration of hydroxyl group. Band at 1640 $cm^{-1}$ can be described as the asymmetric $COO^-$ stretching vibrations. Bands at 1490 and 1385 $cm^{-1}$ can be assigned to the splitting of the $CO_3^{2-}$ asymmetric stretching of metal carbonates. Absorption band near 575 $cm^{-1}$ is due to the combined effect of Ni-O and Mn-O stretching vibrations [10-12].

In order to study the local structure and phonon behavior of the SNMO we have used the Raman spectroscopic measurement at room temperature as shown in Fig. 7. It is observed from the XRD analysis that SNMO are crystallized in monoclinic $P2_1/n$ space group ($C^5_{2h}$), where the Ni and Mn ions occupy the 2a and 2b Wyckoff sites of $C_i$ symmetry, and Sm and O ions are at 4e sites of general $C_1$ symmetry. Thus, the zone-center Raman active modes [13] for SNMO having $C^5_{2h}$ point group symmetry are 24 and are defined as:

$$\Gamma = 6T(3A_g + 3B_g) + 6L(3A_g + 3B_g) + 2\upsilon_1(A_g + B_g) + \\ + 4\upsilon_2(2A_g + 2B_g) + 6\upsilon_5(3A_g + 3B_g).$$

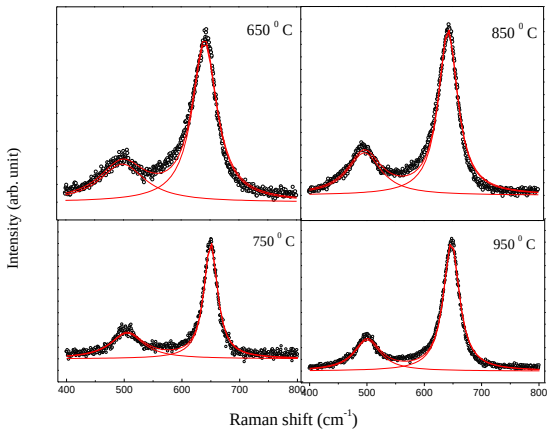


**Fig. 7** – Raman spectra of SNMO

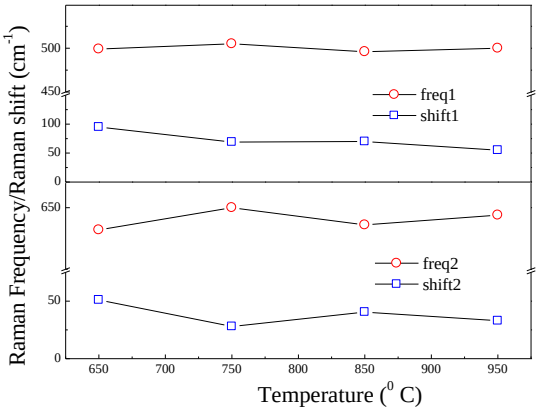


**Fig. 8** – Variation of major peak position and bandwidth with temperature

Here $L$ and $T$ represent the vibrational and translational phonon modes respectively, $\upsilon_1$, $\upsilon_2$ and $\upsilon_5$ correspond to the totally symmetric stretching, antisymmetric stretching and symmetric bending of $NiO_6$ (weak) and/or $MnO_6$ (strong) octahedra. The Raman spectrum of SNMO is well fitted with the sum of Lorentzian peaks (as shown by the solid lines in Fig. 7). Phonon modes at around 641 $cm^{-1}$ can be associated with the stretching (breathing) vibration and at 500 $cm^{-1}$ they are due to the combination of anti-stretching and bending motion of the $(Ni/Mn)O_6$ octahedra [14]. It is seen that with the change of sintering temperature there is a change of sharpness and resonance frequency in the Raman lines. The variation of frequency and width of the peaks is shown in Fig. 8. The Raman active mode frequency for both peaks is less when temperature is 650 °C and 850 °C. The lattice parameters and consequently the cell volume are less for the temperature values. Less cell volume means less space for the octahedral to vibrate. So, frequency is less. The line width of a simple phonon line is a measure of the phonon lifetime. It is determined by the dominating scattering mechanism, which could be temperature independent scattering from lattice defect or temperature dependent scattering from phonons [4]. In the case of bulk material, we get a sharp peak corresponding to zone center phonon only. But in case of nanocrystalline material non-zone center phonon will participate in scattering leading to broadening of the peak. As the cell volume is less for SNMO sintered at 650 and 850 °C, there is more phonon confinement and more broadening.

## 4. CONCLUSIONS

In the present work we have demonstrated through structural investigation the double perovskites SNMO synthesized by simple sol-gel method. From the Reitveld refinement data it is seen that with the change in sintering temperature there are changes in lattice parameters of the SNMO. UV-Visible absorption spectra of the samples reveal that there is a wide variation of band gap and the band gap decreases with the increase of sintering temperature. PL and FTIR spectra are more stable with the change in sintering temperature. Band around 641 $cm^{-1}$ is assigned to stretching (breathing) vibrations, whereas mode near 500 $cm^{-1}$ is mixed type involving both anti stretching and bending. Samples sintered at 650 and 850 °C have reduced cell dimension, which incorporates extra stress and prohibits the octahedral vibration. So frequency of Raman vibration is less for this sample. Broadening of the samples is more for above samples due to quantum confinement effect.

## ACKNOWLEDGEMENTS

Md.S. Sheikh would like to thank Department of Science and Technology (DST), Government of India for providing the financial support in the form of DST INSPIRE Fellowship (IF150220).

## REFERENCES

1. G. King, P.M. Woodward, *J. Mater. Chem.* **20**, 5785 (2010).
2. L.A. Khalam, M.T. Sebastian, *J. Am. Ceram. Soc.* **90** No 5, 1467 (2007).
3. J.B. Goodenough, *Rep. Prog. Phys.* **67**, 1915 (2004).
4. M.N. Iliev, M.M. Gospodinov, M.P. Singh, J. Meen, K.D. Truong, P. Fournier, S. Jandl, *J. Appl. Phys.* **106**, 023515 (2009).
5. Md.S. Sheikh, D. Ghosh, A. Dutta, S. Bhattacharyya, T.P. Sinha, *Mater. Sci. Eng. B* **226**, 10 (2017).
6. Md.S. Sheikh, A.P. Sakhya, R. Maity, A. Dutta, T.P. Sinha, *Sol. Energ. Mater. Sol. C.* **193**, 206 (2019).
7. J. Rodriguez-Carvajal, *Physica B* **192**, 55 (1993).
8. J. Tauc, R. Grigorovici, A. Vancu, *phys. status solidi*, **15**, 627 (1966).
9. D.K. Pandey, A. Modi, P. Pandey, N.K. Gaur, *J. Mater. Sci.: Mater. Electron.* **28** No 22, 17245 (2017).
10. M.P. Reddy, R.A. Shakoor, A.M.A. Mohamed, *Mater. Chem.*

*Phys. Chem.* **177**, 346 (2016).
11. C. Li, B. Liu, Y. He, C. Lv, H. He, Y. Xu, *J. Alloy. Compd.* **590**, 541 (2014).
12. V.M. Gaikward, K.K. Yadav, S.E. Lofland, K.V. Ramanujadrary, S. Chakraverty, A.K. Ganguli, M. Jha, *J. Magn. Magn. Mater* **471**, 8 (2019).
13. D.L. Rousseau, R.P. Bauman, S.P.S. Porto, *J. Raman Sepctrosc.* **10**, 253 (1981).
14. Md.G. Masud, H. Sakata, A.K. Biswal, P.N. Vishwakarma, B.K. Chaudhuri, *J. Phys. D: Appl. Phys.* **48**, 375504 (2015).

## Оптичні та коливальні властивості наночастинок $Sm_2NiMnO_6$ в залежності від температури спікання

R. Mukherjee[1], Md.S. Sheikh[2], T.P. Sinha[2]

[1] *Department of Physics, Ramananda College, Bishnupur, Bankura, 722122, India*
[2] *Department of Physics, Bose Institute, 93/1 A. P. C. Road, Kolkata-700009, India*

Оксиди подвійних перовскітів (DPOs) є цікавими матеріалами завдяки своїм різноманітним важливим технологічним властивостям. Рідкоземельні наночастинки DPO $Sm_2NiMnO_6$ (SNMO) готують методом золь-гелю. Залежно від температури спікання у діапазоні 650-950 °C синтезуються чотири типи матеріалів. Рентгенівські дифрактограми (XRD) кімнатної температури показують, що всі зразки мають найвищий пік інтенсивності під кутом Брегга приблизно $2\theta = 33{,}05°$. Уточнення Рітвельда XRD зразків вказує, що усі матеріали кристалізуються у просторову групу $P2_1/n$.Незважаючи на моноклінну симетрію з однаковою просторовою групою для зразків, мають місце зміни параметрів решітки, об'єму кристала, довжин зв'язків та кутів зв'язків зі зміною температури спікання. Ширину забороненої зони матеріалів отримано з використанням співвідношення Таука для ультрафіолетових спектрів, і виявляється, що вона змінюється від 1,2 до 1,41 еВ. Спектри випромінювання фотолюмінесценції (PL) зразка вимірюються при різних довжинах хвиль збудження. Спектри PL та особливості випромінювання залежать від довжини хвилі збудження. Інфрачервоні спектри з використанням перетворення Фур'є (FTIR) матеріалів несуть у собі структуру подвійного перовскіту. Сильний пік поглинання при 575 $см^{-1}$ у спектрах FTIR зумовлений комбінованим впливом коливань розтягування Ni-O та Mn-O. Спектри комбінаційного розсіювання зразків, узятих на довжині хвилі 488 нм, аналізуються для отримання коливальних режимів зразків. Лоренцові лінії використовуються для відповідності спектрам комбінаційного розсіювання. Групове теоретичне дослідження проводиться для встановлення різних коливальних режимів зразків відповідно до структурної симетрії. Фононні режими, що з'явилися на 641 $см^{-1}$, зумовлені коливаннями розтягування (дихання), а режими на 500 $см^{-1}$ – завдяки поєднанню антирозтягування та руху згину $(Ni/Mn)O_6$ октаедра. Зміни частоти та ширини спектрів комбінаційного розсіювання корелюють зі структурними змінами зразків.

**Ключові слова:** Подвійний перовскіт, Рентгенівська дифракція, Уточнення Рітвельда, Комбінаційне розсіювання світла.